Revista Argentina de Clínica Psicológica
2021, Vol. XXX, N°2, 457-465
DOI: 10.24205/03276716.2020.4045

Influence of low-Frequency High-Magnitude external stimulation on bone healing in a finite elements model

Bojie Chen, Zhongming Huang, Yun Zhang*, Zhengyu Liu, Rui Qian, Shiwei Liu

Abstract

Background: Local mechanical load may affect the long bone fracture heating outcome. But it remains unclear about how the application of external mechanical stimuli affects bone healing. The current study aimed to investigate effects of low-frequency and high magnitude mechanical stimulation on bone healing by finite elements models (FEMs), and trying to define the optimum magnitude and frequency combination improvement in the fracture healing process.

Methods: This study adopted the human tibia finite element model that had callus and a 1.5-mm fracture gap for simulating tissue differentiation in the normal process of fracture healing. Loads were applied at diverse magnitudes and frequencies. Simulation was carried out to predict the major fracture healing processes.

Results: The differentiation of bone callus from fibrous tissue to immature bone tissue was significantly increased with load magnitude from 100N to 300N, while frequency variables did not show a simple dose-response relationship. There existed a significant difference in mature bone tissue element number in loading stimulation with 1Hz and 200N compared with combined loading frequency and magnitude.

Conclusions: Low frequency and high magnitude mechanical stimulus directly affected fracture callus tissue differentiation during bone healing, which provided bases for exploring fracture healing mechanism for fractured bone healing assessment.

Keywords: Fracture healing; Finite Element models; Tissue differentiation; Mechanical load

Introduction

Fracture healing represents a complicated process comprising progressive supporting tissue formation, including mature/immature bone, cartilage, and fibrous connective tissue. In addition, the status of local mechanical loading has been suggested as a potent determining factor for bone formation and tissue differentiation [1]. Loading factors like frequency, magnitude, loading duration and rate exert vital parts in bone formation ability of mechanical loading [2, 3].

However, the mechanical influence of low-frequency and high-magnitude combination on healing outcome was still not investigated. This work focused on investigating how high-magnitude and low-frequency mechanical stimulation affected the bone healing processes, as well as to determine the optimum magnitude-frequency combination for improving the process of fracture healing.

Department of Joint Surgery, The Affiliated Ganzhou Hospital of Nanchang University, Ganzhou, Jiangxi 341000, P.R. China.
Correspondence information: Yun Zhang, Department of Joint Surgery, The Affiliated Ganzhou Hospital of Nanchang University, No.16 Meiguan Avenue, Zhanggong District, Ganzhou, Jiangxi 341000, P.R. China.
Tel: 86-15079794910; Fax: 86-07975889774; E-mail: cbj890410@163.com.

Literature Review

Numerous studies [4-6] have attempted to analyze those parameters of mechanical loading affecting tissue differentiation, by employing either experimental or computational models. As revealed by previous studies, applying the low-magnitude (frequency, 5-40 Hz) external cyclic mechanical stimulus may improve the process of bone healing [7-9]. In addition, some studies have computationally examined how external load frequency affects mechanical stimulus within callus [10, 11] for determining the impacts of high-frequency and low-magnitude mechanical stimulation on the outcome of fracture healing. Similarly, Lacroix and Prendergast [12] proposed the bone regeneration and tissue differentiation model for simulating the bone healing process at 2 diverse loading magnitudes. However, Gómez-Benito *et al* [13] examined how high-frequency cyclic stimulus affected the healing of bone fracture using experimental and computational analysis of a sheep long bone. As revealed by the collective results of these previous studies, mechanical factors affect fracture healing. The optimum combination of these mechanical factors still remains to be elucidated.

In recent years, several studies have evaluated the effect of biomechanical environment (frequency/magnitude) on fracture healing. According to Scheuren AC et al., local mechanical signals might regulate trabecular bone adaptation in vivo; besides, mechanical regulation was determined by the load frequency from a logarithmic perspective, and frequencies under the optimal threshold had catabolic activity, whereas frequencies higher than the threshold had anabolic activity [14]. Barcik J et al. investigated bone healing using the sheep model at the load frequency of 0.5-2.0 Hz and confirmed the feasibility of the system [15]. Li Y et al. investigated how diverse or successive intermittent high-frequency and low-magnitude vibration regimens affected bone healing using the sheep models based on radiographs, biochemical and mechanical testing. In addition, the biomechanical environment can be applied to plant integration [16]. Li J et al investigated the fixator-bone system deformation and stress by finite element analysis under three loading conditions [17]. Therefore, a proper frequency and magnitude loading are important for promoting fracture healing.

Materials and methods

Equipment and software

This study utilized the 64-row, 128-slice volumetric CT scanner (Siemens, Germany) and Windows7 operating system computer software, Mimics16.0 (Materialise, Belgium), Abaqus 6.13 software (Dassault Systèmes, France).

Model construction

The Ethics Committee from The Affiliated Ganzhou Hospital of Nanchang University approved our study protocols. A healthy male (170 cm height and 70 kg weight) was selected. The volunteer had informed and signed consent without any history of trauma or other diseases. CT scanner (conditions: 120 kV, 250 mA, 0.625 mm slice thickness) was used to scan both lower limbs of the volunteers. The scanning thickness from the ankle joint to the top of the knee joint was 0.65mm. A total of 422 layers of three-dimensional CT images were obtained. In addition, the data obtained from the CT scan were imported into the computer in DICOM format.

FE model

For the finite element model (FEM), we later stored and input CT scans in the format of DICOM and processed them by adopting the Mimics Software (The Materialise, Leuven, Belgium) for generating the 3D model. Subsequently, in the Mimics software, the CAD module was used to simulate the 1.5mm gap transverse fracture model in the middle of the tibia. Then, the same software was employed to design a simplified tibial plate model based on the original data. Therefore, in the experiment, tibia-plate systems went through the assembly of separate tibia, screw and plate models. Tibia-plate systems was imported into the Mimics software Remesh module. When noise was reduced, smoothed, loosened, and locally removed, we output the surface mesh in the format of STL, then transformed it into the Inp file, and input it to the Abaqus. In addition, we produced the 3D FEM for tibia-plate internal fixation by further mesh processing in Abaqus software, and tetrahedral elements were generated respectively. Finally, we suggested that the original callus comprised the granulation tissue within the fracture fragment by simulating with Abaqus software.

Material properties

Abaqus 6.13 was adopted for FE analysis. Meanwhile, we carried out map meshing of the model with the 4-node 3D tetrahedral elements for guaranteeing the great consistency and mesh quality. The number of initial callus elements was 12,709. There were 81,970 and 368,784 external fixator and cortical bone elements, separately, which were later modeled in the linear elastic materials. The callus tissue was regarded as homogeneous, sotropic and linearly elastic, while it was suggested that the whole callus comprised granulation tissues when starting the stimulation regimen. Additionally, we simulated the 1.5 mm fracture gap with an even callus and deemed the callus index as 1.4. Four types of biological material were included into bone healing modeling, including cartilage, fibrous tissue, mature and immature bones. Table I presents properties of related materials [18].

Loading and boundary conditions

For completing model definition, we imposed the loading and boundary conditions. The bone proximal cortex was subjected to the symmetric axial compressive load, whereas its distal end interface was constrained in all degrees of freedom (DOF) by using the Abquas software (Fig. 1). The effect of cyclic stimulation on fracture healing was examined. The following mechanical parameters were tested. Loading was performed at one of five frequencies (0.5, 1.0, 1.5, 2.0 or 3.0 Hz) and one of five load magnitudes (100, 150, 200, 250 or 300 N).

Optimisation algorithm

Bone tissue differentiation in the process of bone healing was simulated by iteration [4], which included i) determining biophysical stimuli for the certain material, geometry and loading properties; ii) predicting the mechanical-regulatory concept (put forward by Isaksson and coworkers)-based tissue differentiation [19] (it considers deviatoric strain as the tissue differentiation mechanical regulators); and iii) renewing the element material properties based on the estimated phenotype as well as the callus tissue differentiation amount. The above three steps were repeated, followed by automatic and continuous prediction of tissue differentiation till reaching the mature bone tissue. The following iteration process was initiated after determining new material characteristics. Since it generally requires 4 months to heal the human tibia, we ran the iterations for 16 times, with one iteration corresponding to 1 week during the bone healing process.

The present study applied the iterative algorithm in simulating tissue differentiation during tibia fracture healing. We employ the "elimination method" to calculate and set the "elimination coefficient" to 5% [20]. An optimum design was acquired through the continuous removal of inefficient homogeneous materials from the great design domain, where the lowly-strained tissues were eliminated out of the great tissue domain, whereas the highly-strained regions were preserved.

Fv233inite element analysis and data acquisition

The first analysis was performed under the load of different mechanical parameters, the internal stress, the interfragmentary movement and strain, the change of the number of bone callus units and the healing pattern obtained by the fracture healing simulation.

Results

The pattern of callus growth and tissue differentiation during healing

Callus morphology was altered in 25 frequency/magnitude combination simulations. Compared with the starting conditions, changes in the shape and size of the callus during the iteration procedure were predicted for 25 load parameter combinations (Fig. 2). In all iterations, numerous elements were eliminated by adopting the algorithm, while just elements undergoing ≥5% stain were left, leading to the element pattern consistent with that in the original strain field. There were complicated changes in mechanical stimuli inside the callus. In addition, each tissue differentiation phase was seen, ranging from fibrous connective tissues to cartilages to bones.

Experimental validation of the FE model at different loading

A 200-N magnitude produced the highest quantity of mature callus tissue. In terms of callus element population, a markedly increased differentiation of sheep bone callus from fibrous tissue into immature bone tissue was observed when frequency was unchanged compared with other loading magnitude. By contrast, mature bone tissue did not exhibit an increased rate of differentiation (Fig. 3). The highest quantity of mature callus tissue was observed at 200 N loading magnitude, while the number of mature callus observed at a magnitude of 250 or 300 N was demonstrated to be reduced. The final callus predicted the generation of small quantities of mature bone in the gap.

Experimental validation of the FE model at different frequency

Bone callus differentiation was not found to markedly depend on the frequency variable when load magnitude was unchanged. In response to the application of varying frequency values, the number of callus elements did not show a simple dose-response association. There was a tendency toward a maximum callus element population between 1.0 and 2.0 Hz. Callus tissue growth and differentiation depended on loading frequency and magnitude. A larger amount of mature bone tissue in the loading stimulation with 1 Hz and 200 N was compared with the combined loading frequency and magnitude. Stimulation with 3 Hz and 300 N load suppresses the above sequence since there are greater amounts of cartilages and fibrous connective tissues at first.

Relationship between local strain, movement and callus stiffness

The interfragmentary strain and movement were calculated under different loading conditions (Fig. 4). Within our loading magnitude and frequency ranges, the interfragmentary strain remarkably decreased with the increase in bone tissue elastic modulus, no matter whether a high or low load was applied. As callus stiffness increased, interfragmentary movement decreased moderately among the simulated cases.

Relationship between local stress and callus

stiffness

At the early bone healing stage, the callus is fibrous connective tissue with low elastic modulus and the internal fixator bears more stress, presenting stress shielding effect. Therefore, the interfragmentary remains relatively stable to help fracture healing. With the progress of the fracture healing process, the fibrous connective tissue with low elastic modulus continuously differentiated into callus tissue with high elastic modulus. The callus elastic modulus increased, and the stress shielding effect of internal fixator gradually decreased, so that the stress could be better conducted to bone tissue of interfragmentary (Fig. 5).

Discussion

In vivo and in vitro results provide evidence for the dependency of fracture healing on the frequency and load magnitude. This study computationally analyzed the fracture callus in the tibia for the sake of determining the impacts of diverse loads under the mechanical condition [20]. In the present study, a bone callus population dynamics model for bone remodeling under mechanical loading was constructed. We simulated the effects of the combination of different load parameters on the callus and compared them with the computational results.

The present results showed that a frequency of 1 Hz and 200 N magnitude was more effective in bone healing compared with other parameter combinations, which may be associated with the dependence of tissue differentiation on loading magnitude. As revealed by the present results, low-frequency loading affected bone formation depending on its magnitude, which might also be applied to the healing of peri-implant bone. Some articles report that the high-frequency loads facilitate bone healing, but no high magnitude is necessary for such stimulating effect [21, 13, 7]. Many studies have suggested that low-frequency (<3 Hz) biophysical stimuli affected bone regeneration and healing [9, 22, 23]. There is evidence to support the hypothesis that the bone shows high sensitivity to the load magnitude at low-frequency, and a greater magnitude exhibits superior bone formation ability.

There are still some limitations in the current study. Firstly, the callus FE mesh represented the simple model for mechanical and geometric behaviors of the callus in vivo. When simulating a gait cycle, an axial force stimulus is applied into cortical bone, while forces applied in the remaining directions are neglected. In addition, muscle loading was excluded. Secondly, we considered those identical mechanical characteristics in each analyzed stimulation regime; thus, healing tissue evolution that may have occurred using different stimulation parameters was not considered. However, this approach did not considerably affect the qualitative evaluation of the various stimuli. Thirdly, strain rate and the number of cycles have previously been found to affect callus size and growth [24, 25], while in this work, we applied static loading, so such factors were not considered in the algorithm. Besides, as for iteration, the sub-structuring method was utilized to calculate biophysical stimuli applied in the tibia, so it might not be accurate when the biophysical stimuli were determined for the entire bone.

In addition, our results indicated the isotropic and linear elastic characteristics of materials, but in reality, these tissues are considered to have poroelastic material properties. As revealed by comparative research, there is just mild difference in callus simulated by adopting the poroelastic and linear elastic materials models. Certain studies have used poroelastic materials for fracture healing simulations, which may interpret time-dependent effects, making it possible to adopt fluid flow to mechanically stimulate tissue differentiation [26-28]. Nonetheless, consistent findings to the real procedure are obtained previously by the use of deviatoric strain under physiological loads [29, 19]. Moreover, previous works also suggest that, fluid flow and pore pressure cannot accurately estimate tissue distribution in the process of bone healing in the presence of axial loading; but experimental results indicate that full healing and bridging can be accurately simulated in the presence of torsional loading, when deviatoric strain and the fluid flow were used as mechanical stimuli [30]. In our study, axial loading was dominant in the load case in the process of simulation, which revealed that it was appropriate to utilize deviatoric strain but not fluid flow to be the mechanical stimulus, and therefore also assumed that the use of poroelastic materials was unnecessary in the present simulations.

In our future work, a comprehensive model encompasses all the phases of healing from inflammation to remodeling will be considered. Both biochemical signals and different external loading mechanics stimuli will be the trends of future modeling. Fixed optimization design is another application. Fractures are usually treated by fixation, which significantly affects callus mechanical stability, which in turn affects the outcome of healing. Therefore, optimizing the modeling of fixation is undoubtedly a necessary condition for good fracture healing. In order to further improve the computational model, it is very important to combine the computational model with the corresponding experiments. Meanwhile, it is of great importance to validate model parameters. By using computational models, it is possible to test those undefined bone healing mechanisms; in this regard, clinicians are able to execute the best therapeutic strategies. Finite element analysis is a simulation of actual situation, there might be some theoretical defects and shortcomings. But the analysis results could be used to guide practical work to a certain extent. The computer operation ability in this study is limited, this topic in the tibia model could not accurately simulate the actual situation of bone modeling accuracy, and the problem of material attribute assignment remains further exploration.

To sum up, our findings in this work indicate that callus tissue growth and differentiation are stimulated by low-frequency loading, and it elevates as the magnitude increases in an appropriate range (<300 N). In this model, the optimal algorithm proposed allows for the automatic simulation of callus tissue formation within the ideal fractures under the optimal loading conditions, thus facilitating to quantitatively analyze how mechanical loading affects the differentiation of bone tissues. For determining the reliability and accuracy of our proposed methods, it is necessary to investigate the complicated fractures under more complicated loading conditions. At last, the above primary findings suggest that our methods can be adopted to predict the healing process in preclinical tests.

Acknowledgements:

The study was supported by a grant from Science and Technology Plan of Jiangxi Provincial Health Commission (no.20204611).

Declaration of Conflict of Interest

None.

References

[1] Epari, D. R., Taylor, W. R., Heller, M. O. & Duda, G. N. (2006). Mechanical conditions in the initial phase of bone healing. *Clinical biomechanics, 21*(6), 646-655.

[2] Turner, C. H. (1998). Three rules for bone adaptation to mechanical stimuli. *Bone, 23*(5), 399-407.

[3] Lipphaus, A. & Witzel, U. (2018). Finite-element syntheses of callus and bone remodeling: Biomechanical study of fracture healing in long bones. *The Anatomical Record, 301*(12), 2112-2121.

[4] Lacroix, D., Prendergast, P., Li, G. & Marsh, D. (2002). Biomechanical model to simulate tissue differentiation and bone regeneration: application to fracture healing. *Medical and Biological Engineering and Computing, 40*(1), 14-21.

[5] Ghimire, S., Miramini, S., Richardson, M., Mendis, P. & Zhang, L. (2018). Role of dynamic loading on early stage of bone fracture healing. *Annals of biomedical engineering, 46*(11), 1768-1784.

[6] Wang, M. & Yang, N. (2018). Three-dimensional computational model simulating the fracture healing process with both biphasic poroelastic finite element analysis and fuzzy logic control. *Scientific reports, 8*(1), 1-13.

[7] Goodship, A. E., Lawes, T. J. & Rubin, C. T. (2009). Low-magnitude high-frequency mechanical signals accelerate and augment endochondral bone repair: Preliminary evidence of efficacy. *Journal of orthopaedic research, 27*(7), 922-930.

[8] Warden, S. & Turner, C. (2004). Mechanotransduction in the cortical bone is most efficient at loading frequencies of 5–10 Hz. *Bone, 34*(2), 261-270.

[9] Zhang, X., Vandamme, K., Torcasio, A., Ogawa, T., Van Lenthe, G. H., Naert, I. & Duyck, J. (2012). In vivo assessment of the effect of controlled high-and low-frequency mechanical loading on peri-implant bone healing. *Journal of The Royal Society Interface, 9*(72), 1697-1704.

[10] Prendergast, P., Huiskes, R. & Søballe, K. (1997). Biophysical stimuli on cells during tissue differentiation at implant interfaces. *Journal of biomechanics, 30*(6), 539-548.

[11] González-Torres, L., Gómez-Benito, M., Doblaré, M. & García-Aznar, J. (2010). Influence of the frequency of the external mechanical stimulus on bone healing: a computational study. *Medical engineering & physics, 32*(4), 363-371.

[12] Lacroix, D. & Prendergast, P. (2002). Three-dimensional simulation of fracture repair in the human tibia. *Computer Methods in Biomechanics & Biomedical Engineering, 5*(5), 369-376.

[13] Gómez-Benito, M. J., González-Torres, L. A., Reina-Romo, E., Grasa, J., Seral, B. & García-Aznar, J. M. (2011). Influence of high-frequency cyclical stimulation on the bone fracture-healing process: mathematical and experimental models. *Philosophical Transactions of the Royal Society A:*

Mathematical, Physical and Engineering Sciences, 369(1954), 4278-4294.

[14] Scheuren, A. C., Vallaster, P., Kuhn, G. A., Paul, G. R., Malhotra, A., Kameo, Y. & Müller, R. (2020). Mechano-regulation of trabecular bone adaptation is controlled by the local in vivo environment and logarithmically dependent on loading frequency. *Frontiers in bioengineering and biotechnology, 8*(

[15] Barcik, J., Ernst, M., Dlaska, C. E., Drenchev, L., Zeiter, S., Epari, D. R. & Windolf, M. (2021). Programable Active Fixator System for Systematic In Vivo Investigation of Bone Healing Processes. *Sensors, 21*(1), 17.

[16] Li, Y., Liu, G., Yu, J., Li, C., Tan, L., Hao, B., Liu, C., Lin, J., Zhu, D. & Zhang, X. (2018). Effects of continuous or intermittent low-magnitude high-frequency vibration on fracture healing in sheep. *International orthopaedics, 42*(4), 939-946.

[17] Li, J., Zhao, X., Hu, X., Tao, C. & Ji, R. (2018). A finite element analysis for monitoring the healing progression of fixator-bone system under three loading conditions. *Bio-medical materials and engineering, 29*(4), 473-483.

[18] Byrne, D. P., Lacroix, D. & Prendergast, P. J. (2011). Simulation of fracture healing in the tibia: mechanoregulation of cell activity using a lattice modeling approach. *Journal of orthopaedic research, 29*(10), 1496-1503.

[19] Isaksson, H., Wilson, W., Van Donkelaar, C. C., Huiskes, R. & Ito, K. (2006). Comparison of biophysical stimuli for mechano-regulation of tissue differentiation during fracture healing. *Journal of biomechanics, 39*(8), 1507-1516.

[20] Comiskey, D., Macdonald, B., Mccartney, W., Synnott, K. & O'byrne, J. (2012). Predicting the external formation of a bone fracture callus: an optimisation approach. *Computer methods in biomechanics and biomedical engineering, 15*(7), 779-785.

[21] Wolf, S., Augat, P., Eckert-Hübner, K., Laule, A., Krischak, G. D. & Claes, L. E. (2001). Effects of high-frequency, low-magnitude mechanical stimulus on bone healing. *Clinical Orthopaedics and Related Research®, 385*(192-198.

[22] Sarmiento, A., Mckellop, H. A., Llinas, A., Park, S. H., Lu, B., Stetson, W. & Rao, R. (1996). Effect of loading and fracture motions on diaphyseal tibial fractures. *Journal of orthopaedic research, 14*(1), 80-84.

[23] Yao, J.-F., Shen, J.-Z., Li, D.-K., Lin, D.-S., Li, L., Li, Q., Qi, P., Lian, K.-J. & Ding, Z.-Q. (2012). Rap system of stress stimulation can promote bone union after lower tibial bone fracture: a clinical research. *International journal of medical sciences, 9*(6), 462.

[24] Goodship, A. E., Cunningham, J. L. & Kenwright, J. (1998). Strain rate and timing of stimulation in mechanical modulation of fracture healing. *Clinical Orthopaedics and Related Research®, 355*(S105-S115.

[25] Hente, R., Füchtmeier, B., Schlegel, U., Ernstberger, A. & Perren, S. (2004). The influence of cyclic compression and distraction on the healing of experimental tibial fractures. *Journal of orthopaedic research, 22*(4), 709-715.

[26] García-Aznar, J., Kuiper, J., Gómez-Benito, M., Doblaré, M. & Richardson, J. (2007). Computational simulation of fracture healing: influence of interfragmentary movement on the callus growth. *Journal of Biomechanics, 40*(7), 1467-1476.

[27] Lacroix, D. & Prendergast, P. (2002). A mechano-regulation model for tissue differentiation during fracture healing: analysis of gap size and loading. *Journal of biomechanics, 35*(9), 1163-1171.

[28] Isaksson, H., Van Donkelaar, C. C. & Ito, K. (2009). Sensitivity of tissue differentiation and bone healing predictions to tissue properties. *Journal of biomechanics, 42*(5), 555-564.

[29] Gómez-Benito, M., Garcia-Aznar, J., Kuiper, J. & Doblaré, M. (2005). Influence of fracture gap size on the pattern of long bone healing: a computational study. *Journal of theoretical biology, 235*(1), 105-119.

[30] Isaksson, H., Van Donkelaar, C. C., Huiskes, R. & Ito, K. (2006). Corroboration of mechanoregulatory algorithms for tissue differentiation during fracture healing: comparison with in vivo results. *Journal of Orthopaedic Research, 24*(5), 898-907.

Table 1. **The Properties of some biological materials.**

Tissue type	Elastic modulus in MPa	Poisson's ratio
Granulation tissue	0.2	0.167
Fibrous tissue	2	0.167
Cartilage	10	0.167
Immature bone	1000	0.3
Mature bone	6000	0.3
Cortical bone	17000	0.3
Fixator	200000	0.3

464 Bojie Chen, Zhongming Huang, Yun Zhang, Zhengyu Liu, Rui Qian, Shiwei Liu

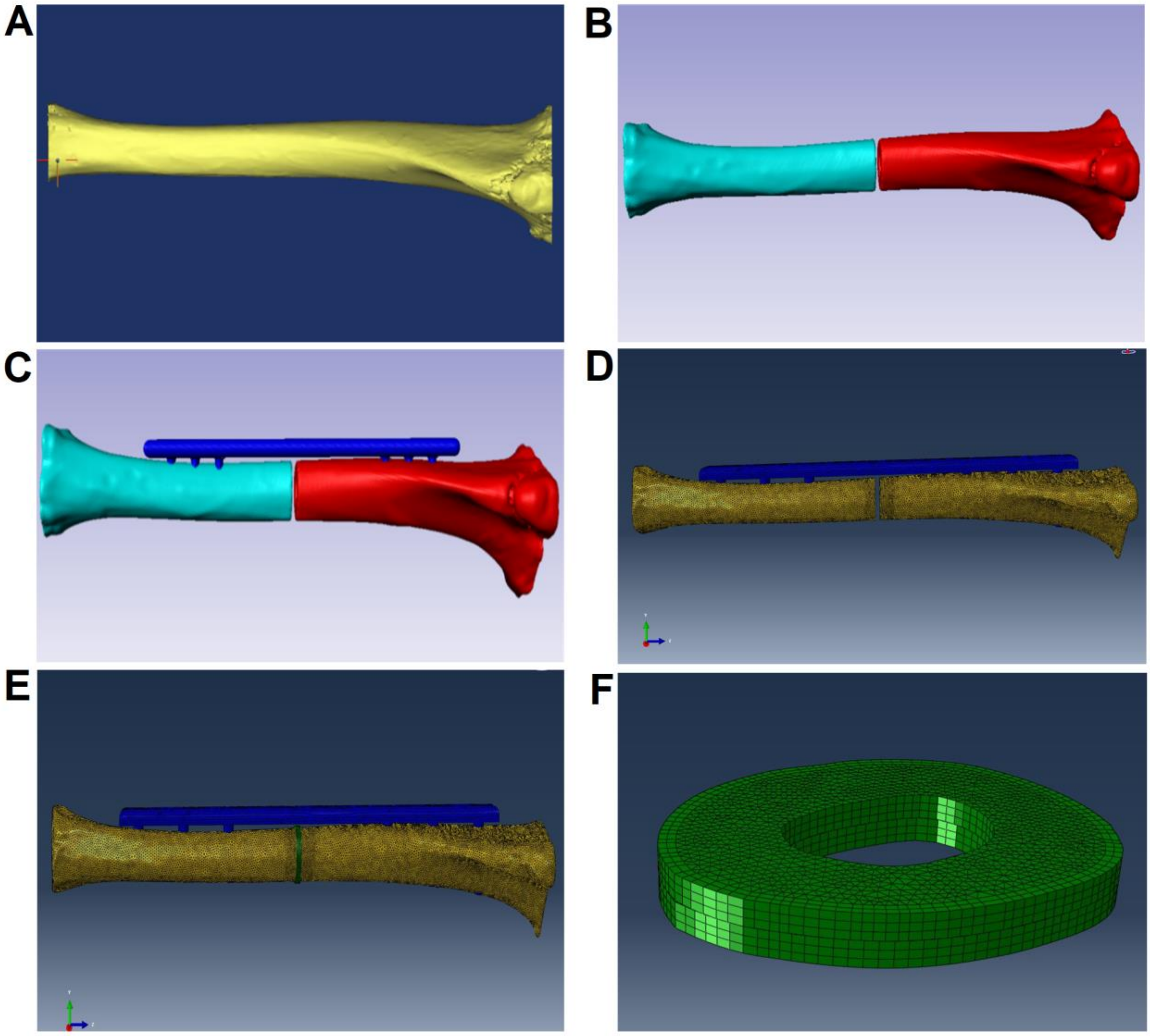

Figures Legends

Figure 1. **3-FE model mesh of the synthetic tibia showing the intact tibia 3D model (A), intact tibia with 1.5mm fracture gap (B), tibia fracture with plate (C), meshes for tibia and implants (D), granulation tissue of fracture fragment (E), and Amplification of granulation tissue (F).**

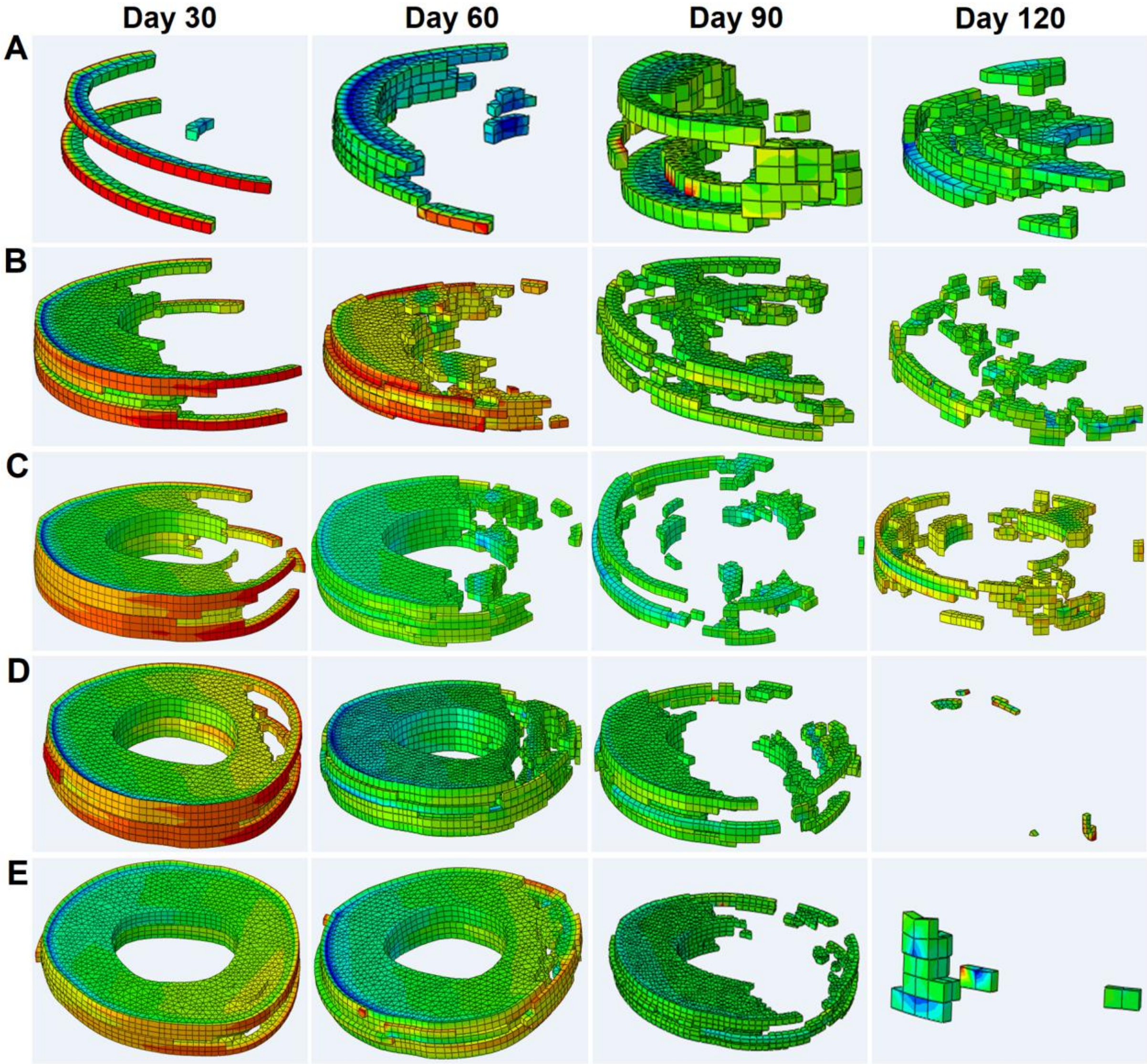

Figure 2. **Callus tissue Simulation view of the predicted healing patterns over time when stimulating with different mechanical stimulus. (A) 100N and 1Hz load, (B) 150N and 1Hz load, (C) 200N and 1Hz load, (D) 250N and 1Hz load, (E) 300N and 1Hz load. (Day30: Fibrous tissue; Day60: Cartilage; Day90: Immature bone; Day120: Mature bone).**

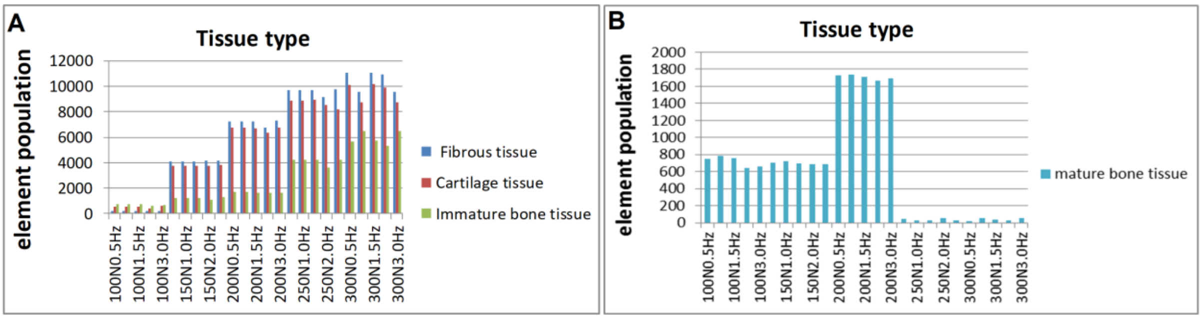

Figure 3. **Element population in Fibrous, Cartilage and Immature bone tissues (A) and mature bone tissues (B) at different frequency and magnitude combination.**

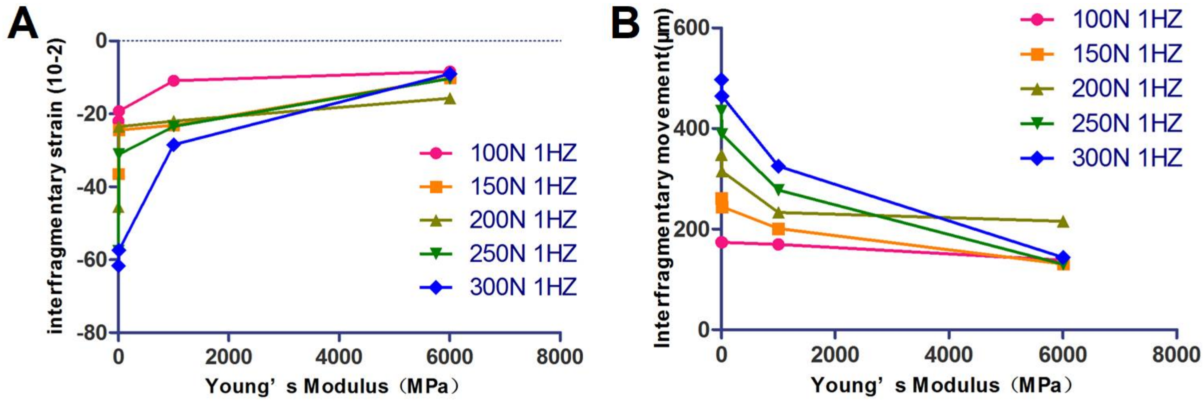

Figure 4. **The interfragmentary strain (A) and movement (B) were calculated under different loading conditions.**

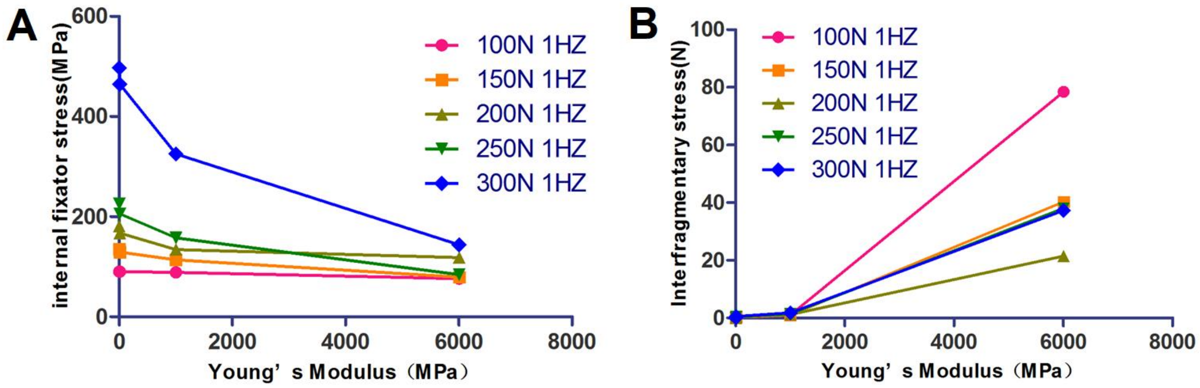

Figure 5. **Relationship between the young's modulus and the internal fixator stress (A) and interfragmentary stress (B).**